Global Solar Radiation of some Regions of Cameroon using the Linear Angstrom Model and Non-linear Polynomial Relations: Part 2, Sun-path Diagrams, Energy Potential Predictions and Statistical Validation

Afungchui David *‡, Ebobenow Joseph** , Neba Rene Ngwa***, Nkongho Ayuketang Arreyndip****

*University of Bamenda, Faculty of Sciences; Department of Physics, PO Box 39, Bambili, NWR, Cameroon

*; ** ; ****University of Buea, Department of Physics, 65 Buea, Cameroon

*** University of Bamenda, HTTC; Department of Physics, PO Box 39, Bambili, NWR, Cameroon

(afungchui.david@ubuea.cm, Ebobenow@gmail.com, ,renereynaldo@gmail.com, ayuketang@aims-cameroon.org)

‡ Corresponding Author; First, Postal address, Tel: +237 654 785 555 Fax: +237 233 366 030 , afungchui.david@ubuea.cm

Received: 06.06.2017 Accepted:24.07.2017

Abstract- This paper aims to use the linear Angstrom model and non-linear polynomial relations to assess the global solar radiation (GSR) of some localities of Cameroon. The computation of the Angstrom correlation coefficients for the implemented models is accomplished using the least square method. These coefficients constitute the basis for predicting the GSR of the chosen geographical locations. The predictions are validated by some versatile statistical methods, which include: the mean bias error (MBE), the mean relative error (MRE), the root mean square error (RMSE) and t-statistic (t-stat) error. The input data for the analyses are the measured GSR and mean number of monthly sun shine hours. The data for the analyses is obtained partly from the archives of National Aeronautics and Space Administration (NASA) and partly from the archives of the Cameroon Department of Meteorology, Douala. The data used spans a period of 23 years. We demonstrate the validity of the developed models by comparing the evaluated values of GSR with the measured ones. Hence the regression equations can be used to confidently predict the GSR of the representative regions in the absence of experimental data. We equally implement a high-precision sun-tracking algorithm which is necessary to follow the sun's trajectory from dawn till dusk, in order to maintain high power output and stability of a solar power system.

Key words- Global Solar Radiation, Angstrom, least square method, regression analysis, sun shine hours, mean bias error (MBE), mean relative error (MRE), root mean square error (RMSE), t-statistic, sun-tracking, sun path diagram.

Nomenclature

GSR	Global Solar Radiation
G_0	Extra-terrestrial radiation
I_{sc}	Solar constant (=1,367W/m^2)
H	Monthly average daily GSR (MJ/m^2-day)
H_0	Monthly average daily extra-terrestrial solar radiation (MJ/m^2-day)
n_{day}	Number of days of the year starting from 1st January
n	Number of observations and corresponds to the twelve months of the year
S	The monthly average daily hours of bright sunshine (h)
S_0	The monthly average of the maximum possible daily hours of bright sunshine (h)
Z	Altitude (m)

T^4 The fourth power of absolute temperature
a, b, c, d Coefficients in empirical correlation relationships

Greek letters

δ Solar declination angle (^{0})
φ Latitude of site (^{0})
ω_s Mean sunshine hour angle for the month (^{0})
$\sum$ Summation

1. Introduction

To ensure a healthy and safe planet free from increasing pollution and to curb down global warming effects, the tendency is to shift from using the traditional fossil fuels, to the environmentally friendly renewable alternatives. Solar energy which is the most abundant energy source promises to be the optimal energy source for the future. Solar energy, though abundantly distributed all-round the year; its share in the Cameroon renewable energy exploitation is minimal. As of present, the rural energy needs for cooking, heating and lighting are satisfied mainly by wood-biomass. Electricity which supplies only about 48% of people and mostly those in urban areas is mainly from hydro power plants [1-2].

The least square method is used derived the Angstrom correlation coefficients for the linear, quadratic and cubic polynomial models, for some chosen geographical locations, based on the local latitude and longitude information. The input data are the measured values of global solar irradiation and sunshine duration hours. The derived linear and non-linear polynomial relations are used to predict the global solar irradiation of the chosen regions even in the absence of experimental data. The predictions are evaluated using: the mean bias error (MBE), the mean relative error (MRE), the root mean square error (RMSE) and t-statistic (t-stat) error.

Regression analyses are performed using sunshine duration as the input parameter to evaluate the daily GSR. This process enables us to determine the different correlation coefficients for some given locations which lead to identifying the best model. The Angstrom models used, are either: in the linear [3-6], or in the modified quadratic [7,8,9] and polynomial [10-11] forms. These have been tested to be adaptable, consistent and viable for solar energy potential assessment under different climatic conditions [3, 7- 22]. The models however depend on locality [7,14,15] and as such there is a need to compute the regression coefficients for different parts of the world. This has led to a substantial volume of literature on the subject given the abundance of solar radiation over the surface of the earth. Even though it would be expected that the higher order polynomial model should provide the best results, it has been established that, the linear Angstrom model has proven satisfactory in some cases while in others it is the quadratic model. Che et al. [10] in addition to the polynomial models successfully used trigonometric functions in conjunction with sine and cosine wave for estimating daily GSR. Different approaches are used in the models. One option is to use the daily duration of sun shine hours and the mean daily GSR data [3, 13]. Another is to use in addition the: mean clearness index, mean daily maximum temperature, mean relative humidity, mean daily sea level pressure, and the mean daily vapour pressure [5,13,16,23,24,59]. Still, artificial intelligence [25,53-54,56,60] or the application of atmospheric optics to meteosat imagery [26,57], are amongst the other successful approaches to estimate the GSR.

The accuracy of the models is established by employing statistical evaluation models like the: mean bias error (MBE), root mean square error (RMSE) and t-tatistics [4, 8, 17, 19-21, 27-32, 55, 58]. These statistical tools blend together to guarantee the reliability and consistency of the models [4].

The first objective of this study is to establish the monthly-average daily GSR for Bamenda, Bertoua, Douala, Ngaoundere and Yaounde, some five regions in Cameroon (Fig. 2) using three polynomial models: the linear, quadratic and cubic Angstrom's models. The correlation coefficients for these localities were derived in part I of this paper [2]. The comparison of the three models with the measured values by using statistical methods: MRE, MBE, RMSE and t-statistics will constitute the first objective of this second part of the study. The second objective is to implement an algorithm to track the sun path in the geographical regions of study.

The best utilization of solar energy will be when the path of the sun can be tracked [49]. Tracking can be done manually, but it is not worth the effort for it will mean that someone should be under the sun with a solar panel constantly changing the position of the panel to be perpendicular to the position of the sun. Moreover, it will be very difficult to locate the position of the sun when there is cloud cover. It is generally known that the sun rises in the East and sets in the West. But in reality, the sun does not rise exactly due east or sets exactly due west always. Instead, the sun may rise further north of east or further south of east, depending on the point of observation on the earth surface. The position of the sun can be determined by finding the angle of elevation from the vertical as viewed by an observer and the angle of azimuth measured horizontally from the geographic north. An algorithm described in [50] is used to compute these two angles. High degree of sun-tracking accuracy is required to ensure that the solar collector is capable of harnessing the maximum solar energy throughout the day. In order to maintain high output power and stability of a solar power system, a high-precision sun-tracking algorithm is necessary to follow the sun's trajectory from dawn until dusk.

2. Solar Radiation Data and Model Development

The GSR can be expressed as a function of average daily sunshine duration as follows:

$$\frac{H}{H_0} = f\left(\frac{S}{S_0}\right) \quad (1)$$

$\boldsymbol{H}$ is the monthly average daily GSR (MJ/m^2), H_0 is the monthly average daily extra-terrestrial radiation (MJ/m^2), $\boldsymbol{S}$ is the monthly average daily measured sunshine duration (h) and

S_0 is the monthly average daily maximum sunshine duration (h). Angstrom [4], developed the first expression of this type using a linear regression equation which was later modified by Page [3], and given by:

$$\frac{H}{H_0} = a + b\left(\frac{S}{S_0}\right) \quad (2)$$

As an extension of this equation and to improve the accuracy, the nonlinear polynomial models, were derived. This form is given as follows (Akinoglu and Ecevit [21]; Ogelman et al. [29]; Samuel [34]; Tarhan and Sari [35]; Tasdemiroglu and Sever [36,-38]; Tiris et al. [39-40]; Ulgen and Hepbasli [41]):

$$\frac{H}{H_0} = a + b\left(\frac{S}{S_0}\right) + c\left(\frac{S}{S_0}\right)^2 + d\left(\frac{S}{S_0}\right)^3 + \cdots \quad (3)$$

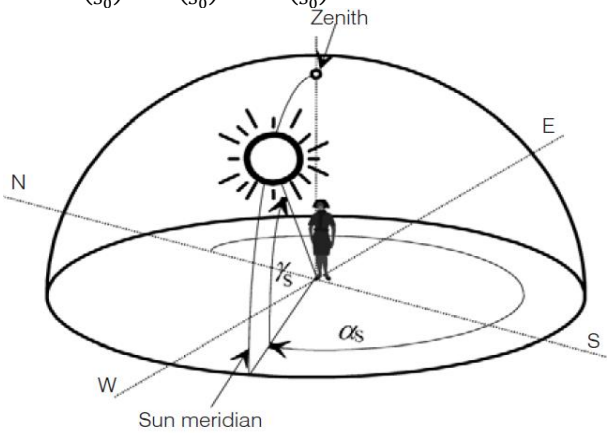

Fig.1. Definition of the angles describing the position of the sun [51]. Where, α_s is the azimuth angle and γ_S is the elevation angle

where ***a, b, c*** and ***d*** are empirical correlation coefficients called Angstrom constants. ***H*** and ***S*** represent the experimental data from solar measurement stations. The values of a, b, c and d, vary depending on location and month of observation. Their values may be affected by atmospheric air pollution resulting from urban activity and factory operation. As the daily total amount of GSR and sunshine duration vary widely from day to day, daily totals averaged over a month are used to derive the values of a, b, c and d.

Experimental data of monthly average GSR for the study were obtained from the archives of NASA [42] while those of sunshine duration in Cameroon were obtained from the archives of the Department of Meteorology (Directorate of National Meteorology) located in Douala recorded over a 23-year period. The geographical parameters and measurement periods for the regions are given in **Table 1** while the regions considered are shown in **Fig. 1.** The monthly measured values of the monthly average daily GSR and sunshine duration are also illustrated in **Tables 2 and 3** respectively.

The monthly average daily extra-terrestrial radiation values on a horizontal surface for the five regions were calculated from the following equations (Iqbal [47]; Kilic and Ozturk [28]):

$$H_0 = \frac{24x3600}{\pi} G_0 \left(\cos\varphi \cdot \cos\delta \cdot \sin\omega_s + \frac{\pi}{180}\omega_s \cdot \sin\varphi \cdot \sin\delta\right) \quad (4)$$

where G_0 is the extra-terrestrial radiation (solar radiation incident outside the earth's atmosphere) and is obtained from:

$$G_0 = I_{sc} \cdot \left(1 + 0.034\cos\left(\frac{360 \cdot n_{day}}{365.25}\right)\right), \quad (5)$$

where I_{sc} is the solar constant and has a value of 1.367 kWm^{-2} (Helwa et al. [37]; Iqbal, [47]), φ is the latitude of the site, δ is the solar declination angle (that is, the angle between a plane perpendicular to a line between the earth and the sun and the earth's axis), ω_s is the sunshine hour angle for the month and n_{day} is the number of days of the year starting from January 1st. For January 1st, $n_{day} = 1$ and for December 31st, $n_{day} = 365$.

The solar declination (δ), the mean sunshine hour angle for the month (ω_s) and the maximum possible sunshine duration (S_0) may be computed from the Cooper [43] formula (Kilic and Ozturk [28]; Duffie and Beckman [44]):

$$\delta = 23.45 sin\left(\frac{360(n_{day}+284)}{365}\right) \quad (6)$$

$$\omega_s = cos^{-1}(-tan\delta \cdot tan\varphi) \quad (7)$$

$$S_0 = \frac{2}{15}\omega_s \quad (8)$$

3. Determination of the Solar Position at a Given Time in a Location

Many sun-tracking algorithms exist. One can integrate one such algorithm in an open loop sun-tracking system. An example is the algorithm that will be used in this paper described in (DIN [50]) as outlined below.

Given the day angle,

$$y' = 360^o . \frac{day\ of\ the\ year}{number\ of\ days\ of\ the\ year}, \quad (9)$$

the solar declination becomes:

$$\delta(y') = \{0.3948 - 2.3.2559.cos(y' + 9.1^o) - 0.3915.cos(2y' + 5.4^o) - 0.1764.cos(3y' + 105.2^o)\}^o \quad (10)$$

and the equation of time,

$$eqt(y') = [0.0066 + 7.3525.cos(y' + 85.9^o) + 9.9359.cos(2.y' + 108.9^o) + 0.3387.cos(3.y' + 105.2^o)]min, \quad (11)$$

is calculated. With the Local time, the Time zone and the longitude λ, the mean local time MLT becomes:

$$\text{MLT} = \text{Local time} - \text{Time zone} + 4 \bullet \lambda \bullet \text{min}/^\circ \quad (12)$$

Adding the equation of time, eqt, to the mean local time MLT provides the Solar time:

$$\text{Solar time} = \text{MLT} + \text{eqt} \quad (13)$$

With the latitude ϕ of the location and the hour angle ω:

$$\omega = (12.00\ \text{h} - \text{Solar time}) \bullet 15^\circ/\text{h} \quad (14)$$

the angle of solar altitude (sun height), γ_S, and angle of solar azimuth, α_S, become:

$$\gamma_S = \arcsin(\cos\omega \bullet \cos\phi \bullet \cos\delta + \sin\phi \bullet \sin\delta) \quad (15)$$

$$\alpha_S = \begin{cases} 180^o - \arccos\frac{\sin\gamma_S.\sin\varphi_S - \sin\delta}{\cos\gamma_S.\cos\varphi} & \text{if Solar time } \leq 12.00 \text{ h} \\ 180^o + \arccos\frac{\sin\gamma_S.\sin\varphi_S - \sin\delta}{\cos\gamma_S.\cos\varphi} & \text{if Solar time } > 12.00 \text{ h} \end{cases} \quad (16)$$

Table 1. Geographical parameters and measurement periods for the five regions considered in Cameroon.

Location	Latitude (^{0}N)	Longitude(^{0}E)	Altitude(m)
Bamenda	5.56	10.15	1400
Bertoua	4.58	13.68	720
Douala	4.06	9.71	2
Ngaoundere	7.32	13.58	1200
Yaounde	3.87	11.52	720

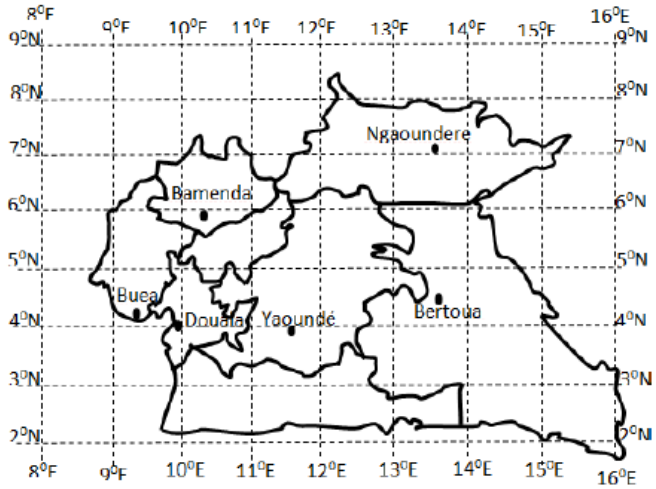

Fig. 2. Region of study

Table 2. Measured values of the monthly average daily GSR on a horizontal surface for five regions of Cameroon in MJ/m^2/day

Months	Location					Monthly average daily values
	Bamenda	Bertoua	Douala	Ngaoundere	Yaounde	
January	23.004	22.860	20.484	23.076	21.276	22.140
February	23.616	23.616	20.808	24.444	22.068	22.896
March	21.348	21.060	18.864	23.400	20.124	20.952
April	19.008	19.584	17.712	20.304	18.612	19.044
May	18.000	18.144	17.100	19.080	17.244	17.928
June	16.452	16.632	15.840	17.640	16.416	16.596
July	15.192	15.444	14.148	16.020	15.948	15.336
August	15.012	15.912	13.500	16.092	16.344	15.372
September	15.768	16.884	14.652	17.244	17.064	16.308
October	16.668	17.064	14.868	18.504	16.488	16.704
November	20.160	19.836	16.884	21.960	18.000	19.368
December	22.032	21.636	19.224	22.464	19.872	21.060

Source: Archives of National Aeronautics and Space Administration (NASA)

Table 3: Measured values of the monthly average daily sunshine duration for the five locations of Cameroon in hours per day

Months	Location					Monthly average daily values
	Bamenda	Bertoua	Douala	Ngaoundere	Yaounde	
January	8.9194	5.1968	8.4161	9.2097	5.7774	7.5032
February	9.4643	6.3357	8.6250	9.2214	6.4500	8.0179
March	8.5323	5.6258	6.9516	7.2677	5.3226	6.7387
April	7.7067	6.1367	6.5833	5.6433	5.6233	6.3400
May	7.9484	6.6355	6.7581	5.8258	5.5484	6.5419
June	6.7000	4.8500	5.9267	4.9400	4.2167	5.3267
July	5.8839	3.3645	3.8323	3.8129	3.3452	4.0484
August	5.2871	2.6774	3.8000	3.3129	2.6387	3.5419
September	6.1533	3.7933	4.3167	4.1500	3.3900	4.3600
October	8.3452	4.5484	5.9258	5.3742	4.1806	5.6742
November	9.2800	6.1467	4.6100	8.6667	5.9000	6.9200
December	9.4226	5.6968	8.7387	9.5774	6.0903	7.9065

Source: Archives of the Department of Meteorology, Douala

4. Determination of the Regression Parameters: a, b and c

The models used to determine the parameters **a, b and c** include: the linear Angstrom-Prescott equation, the modified second order quadratic equation and a polynomial equation of third order. These three models are developed from equation (3) in which the order of the polynomial equation is successively taken to be 1, 2 and 3 respectively. A succinct presentation of these three models was presented in part one of this paper. The method of choice was the least square method. The regression coefficients for the three models are presented in tables 4 to 6.

Table 4. Regression coefficients using the linear model (model1)

Location	**a**	**b**
Bamenda	0.0826	0.6835
Bertoua	0.2861	0.5791
Douala	0.2530	0.4266
Ngaoundere	0.3025	0.4844
Yaounde	0.3142	0.4785

Table 5. Regression coefficients using the quadratic model (Model 2)

Location	**a**	**b**	**c**
Bamenda	0.5396	-0.8253	1.1944
Bertoua	0.1665	1.2340	-0.8444
Douala	0.2990	0.2375	0.1793
Ngaoundere	0.2120	0.8502	- 0.3254
Yaounde	0.5619	1.2454	-0.9684

Table 6. Regression coefficients using the cubic model (Model 3)

Location	**a**	**b**	**c**	**d**
Bamenda	0.4240	- 0.1695	0.0024	0.6947
Bertoua	1.0758	- 6.6503	20.7825	- 18.883
Douala	- 0.6034	5.9653	- 11.3126	7.3260
Ngaoundere	0.2770	0.4270	0.5306	- 0.5374
Yaounde	0.5172	- 0.5617	0.9345	0.7000

Based on the regression coefficients of tables 4 to 6, a procedure for estimating the Monthly average daily GSR on a horizontal surface based on equations (4) to (8) is presented in part I of this paper [2].

5. Statistical Comparison Methods

The prediction efficiencies of the models used are tested using the following methods: mean bias error (MBE), mean relative error (MRE), root mean square error (RMSE) and t-statistic (t-stat) error, which are the most widely used ones.

5.1 Mean Bias Error

The mean bias error (MBE) provides information on the long-term performance of an equation (the correlations) by allowing a comparison of the actual deviation between calculated and measured values term by term. The ideal value of MBE is zero. A positive MBE represents an over-estimation while a negative MBE shows under-estimation. The smaller the MBE value, the better the model's performance. The MBE is given by (Ma and Iqbal [47], Tiris et al. [40]):

$$MBE = \frac{1}{k}\sum_{i=1}^{k}(y_i - x_i) \quad (17)$$

where x_i is the i^{th} measured value, y_i the i^{th} calculated value and k the total number of observations.

5.2 Root Mean Square Error

The root mean square error (RMSE) provides information on the short-term performance of an equation. The RMSE is a frequently used measure of the differences between values predicted by a model or an estimator and the values actually observed or measured from the quantity being modeled or estimated. The smaller the RMSE value, the better the model's performance. RMSE is a good measure of precision and its value is always positive, representing zero in the ideal case (Ma and Iqbal [47]). However, a few large errors in the sum can produce a significant increase in RMSE. The RMSE may be computed from the following equation (Ma and Iqbal [47], Tiris et al. [40]):

$$RMSE = \sqrt{\frac{1}{k}\sum_{i=1}^{k}(y_i - x_i)^2} \quad (18)$$

5.3 Mean Relative Error

The mean relative error (MRE) can also be used as a test for determining the linear relationship between measured and estimated values. The MRE may be computed from the following equation (Bulut and Buyukalaca [48]);

$$MRE = \frac{1}{k}\sum_{i=1}^{k}\left|\frac{y_i - x_i}{x_i}\right| \quad (19)$$

Mean relative error values are always positive, reducing to zero for the ideal case. The smaller the MRE value, the better the model's performance.

It is obvious that each test by itself may not be an adequate indicator of a model's performance. It is possible to have a large RMSE value and at the same time a small MBE (a large scatter about the line of estimation). It is also possible to have a relatively small RMSE and a relatively large MBE (consistently small over-estimation or underestimation).

Table 7. Measured Monthly Average global radiation H, compared with those calculated using Models 1, 2 and 3 for the location of Yaounde.

Months	H measured	H_0	S	S_0	H/H_0	S/S_0	Model 1	Model 2	Model 3
Jan	21.276	35.4827	5.7774	11.6852	0.5996	0.4944	19.5428	19.6003	19.6045
Feb	22.068	37.1166	6.4500	11.9212	0.5946	0.5411	22.2721	22.1673	22.1874
Mar	20.124	37.7134	5.3226	12.0327	0.5336	0.4423	19.8312	19.2971	19.3147
April	18.612	36.7248	5.6233	12.1345	0.5068	0.4634	19.6822	19.3533	19.3628
May	17.244	35.2760	5.5484	12.2078	0.4888	0.4545	18.7555	18.3551	18.3671
June	16.416	34.8750	4.2167	12.2214	0.4707	0.3450	16.7150	16.1109	16.1606
July	15.948	35.8270	3.3452	12.1696	0.4451	0.2749	15.9695	16.0284	16.0487
Aug	16.344	37.0704	2.6387	12.0736	0.4409	0.2186	15.5251	16.6282	16.5475
Sept	17.064	37.1451	3.3900	11.9655	0.4594	0.2833	16.7063	16.6481	16.6777
Oct	16.488	35.7694	4.1806	11.8610	0.4610	0.3525	17.2720	16.6175	16.6678
Nov	18.00	34.2537	5.9000	11.7915	0.5255	0.5004	18.9640	19.1036	19.1079
Dec	19.872	34.0434	6.0903	11.7797	0.5837	0.5170	19.1182	19.5104	19.5176
MRE							0.0422	0.0318	0.0314
MBE							-0.0086	-0.0031	0.0093
RMSE							0.9198	0.7641	0.7603
t-stat							0.0309	0.0134	0.0404

Although these statistical indicators generally provide a reasonable procedure to compare models, they do not objectively indicate whether a model's estimates are statistically significant, that is, not significantly different from their measured counterparts. In this study, an additional statistical indicator, the t-statistic was used. The statistical indicator allows models to be compared and at the same time indicate whether or not a model's estimates are statistically significant at a particular confidence level (Stone 1993[14]). It was seen that the t-statistic used in addition to the RMSE and MBE gave more reliable and explanatory results (Togrul [30]).

5.4 t-statistic Method.

After an estimation of a coefficient, the t-statistic (t-stat) for that coefficient is the ratio of the coefficient to its standard error. In the literature, Stone [14] demonstrated that MBE and RMSE separately do not represent a reliable assessment of the model's performance and can lead to the false selection of the best model from a set of candidates. To determine whether or not the equation estimates are statistically significant, Stone [14] proposed t-stat as:

$$t-stat = \sqrt{\frac{(n-1)MBE^2}{RMSE^2-MBE^2}} \quad (20)$$

t-stat values are always positive and the smaller the value of t, the better is the model's performance. n, represents the numbers of observations and corresponds to the twelve months (n=12) of the year in this study.

6. Results and Discussions

6.1 Comparison for Yaounde

The table 7 shows the values of measured monthly average global radiation (MJ/m2/day) compared with those estimated from Models 1, 2 and 3 for the location of Yaounde.

Upon comparing the results, it can be seen that model 3 has the smallest MRE (0.0314) and RMSE (0.7603) while Model 2 has the smallest MBE (-0.0031) and t-stat value (0.0134). According to the results, Models 2 and 3 are proposed for the estimation of horizontal GSR for Yaounde, with estimates of Model 2 being most statistically significant as seen from their t-stat value. Model 1 has low error values and can also be used for the estimation of the GSR for Yaounde.

Table 8. Statistical Comparison test for the Models 1, 2 and 3 for the different locations

Bamenda			
Stat. method	Model 1	Model 2	Model 3
MRE	0.0237	0.0172	0.0178
MBE	-0.0832	-0.0018	-0.0105
RMSE	0.5456	0.4357	0.4602
t-stat	0.5116	0.0133	0.0759

Bertoua			
Stat. method	Model 1	Model 2	Model 3
MRE	0.0248	0.0308	0.0176
MBE	-0.2387	-0.1553	-0.1551
RMSE	0.6417	0.7646	0.7287
t-stat	1.3289	0.6879	0.7224

Douala			
Stat. method	Model 1	Model 2	Model 3
MRE	0.0278	0.0272	0.0372
MBE	0.0128	0.0144	0.0024
RMSE	0.6241	0.6281	0.6695
t-stat	0.0678	0.0762	0.0120

Ngaoundere			
Stat. method	Model 1	Model 2	Model 3
MRE	0.0178	0.0132	0.0126
MBE	-0.007	-0.0039	-0.0023
RMSE	0.4378	0.3110	0.2812
t-stat	0.0530	0.0418	0.0265

6.2 Comparison for the other geographical regions studied

In order to minimize space, results for the other regions of interest are computed similarly, and summarized in tabular form, in the next section. Only the values of MRE, MBE, RMSE and t-stat (MJ/m^{2}day) for Models (1 to 3) have been tabulated.

Table 8. shows the values of MRE, MBE, RMSE and t-stat (MJ/m^{2}day) for Models (1 to 3) for the different locations.

6.2.1 Comparison for Bamenda

Comparing the results for Bamenda, highlights Models 2 and 3 as best choices for the estimation of the GSR for Bamenda. The estimates of Model 2 being more statistically significant than those of Model 3 as seen from their t-stat values. Model 2 is thus found to be the most accurate for the estimation of the GSR on the horizontal surface for Bamenda. The MRE, MBE, RMSE and t-stat are calculated to be 0.0172, -0.0018, 0.4357 and 0.0133MJ/m^{2}day respectively.

6.2.2 Comparison for Bertoua

Comparing the results, it can be established that some models give good results. Model 3 has the smallest MRE (0.0176) and MBE (-0.1551) than the other models. Model 1 has the smallest RMSE (0.6417) while Model 2 has the smallest t-stat value (0.6879). According to the results, Models 2 and 3 are proposed for the estimation of GSR for Bertoua, with estimates of Model 2 being more statistically significant than those of Model 3 as seen from their t-stat values.

According to the results, Model 3 is found to be the most accurate while Model 2 is most statistically significant for the estimation of the GSR on the horizontal surface of Bamenda.

6.2.3 Comparison for Douala.

For this location, it can be seen that all models give good results. Model 3 has the smallest MBE (0.0024) and t-stat value (0.012) than the other models. Model 1 has the smallest RMSE (0.6241) while Model 2 has the smallest MRE (0.0272). According to the results, Models 1, 2 and 3 are proposed for the estimation of GSR for Douala, with estimates of Model 3 being the most statistically significant than those of the other models as seen from their t-stat values.

6.2.4 Comparison for Ngaoundere

A Comparison of the results in this case reveal, Model 3 has the smallest MRE, MBE, RMSE and t-stat values than the other models. Models 3 is then the best proposal for the estimation of the GSR for Ngaoundere, with estimates being most statistically significant than those of Models 1 and 2, as seen from their t-stat values. The MRE, MBE, RMSE and t-stat are calculated to be 0.0126, -0.0023, 0.2812 and 0.7224 MJ/m^{2}day respectively for Model 3. Models 1 and 2 also have low error values and can also be used for the estimation of horizontal GSR for Ngaoundere.

Based on data in Table 7, the linear relationship between the monthly average values of H/H_0 versus S/S_0 for Yaounde is shown in Fig. 3. The calculated H_0 values for Yaounde were between 34.0434 and 37.7694 MJ/m^{2}day, as such a graph of H_0 was added to the study as shown in Fig. 4.

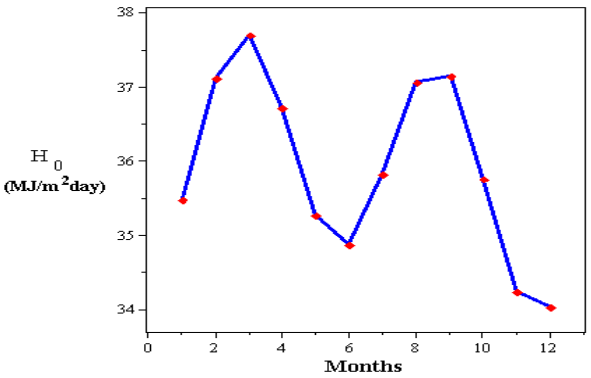

Fig. 3. Linear relationships between the monthly average values (H/H_0 versus S/S_0)

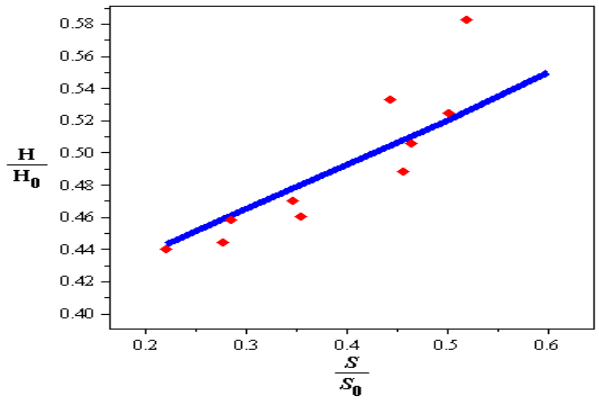

Fig. 4. The monthly average daily extraterrestrial radiation H_0 (MJ/m^2day)

The comparisons of the values of the monthly average GSR measured and calculated from the Models (1, 2, and 3) for Yaounde are shown in Fig. 5.

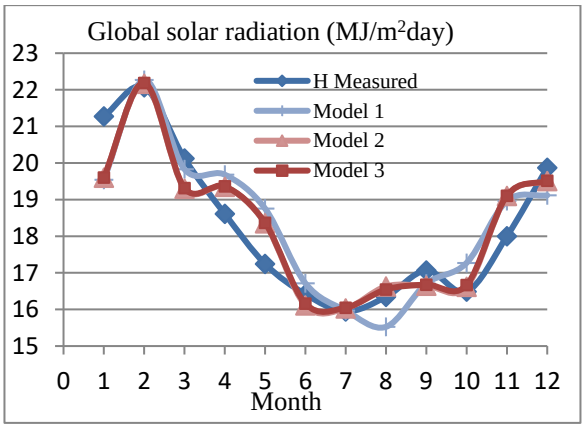

Fig. 5. Comparison of the estimated and observed monthly average daily horizontal GSR data for Yaounde using the three models.

As observed from Fig. 5, the location of Yaounde experienced a decrease in the horizontal GSR from March through August (during the rainy season), with the lowest value of the monthly average mean horizontal global radiation of 15.948MJ/m2day recorded in July (7th month). During the commencement of the dry season (September to October) the location of Yaounde experienced a gradual increase in solar radiation, followed by a decrease in October and then by a rapid increase from November. This same trend is followed in the other regions studied.

6.3 Validation of the coding results of the solar position algorithm

The results generated from the equations (9) to (16) are compared and validated with those from sunearthtools [52] as presented in the table 9.We observe a very close agreement of the results obtained in this paper, for both the solar elevation and azimuth angles, with those from the professional site, sunearthtools [52]. This ascertains the validity of the results and we can then proceed to determine very precisely the solar positions over different geographical locations as the next result show.

6.4 Sun position for Bamenda

The coordinates of Bamenda are 5° 56' 0" North, 10° 10' 0" East. On 29/04/2016, at 2:00 pm, running the program with the following information. The elevation angle: 63.1245°, and the azimuth angle: 290.786°.

The path of the sun in the course of the day can be visualized using sun-path diagrams. These diagrams show sun height and azimuth for every hour of the selected days with a curve drawn through the points. The sun-path diagrams for Bamenda on the 21st of the month of January, February and March in the year 2016 is drawn in Fig. 6.

Table 9. Sun track over a day validated by results from sunearthtools [52]

Date:	25/03/2016 | GMT-5	
Coordinates:	40.76, -73.984	
location:		
hour	Elevation	Azimuth
05:50:13	-0.833°	86.53°
6:00:00	1.02°	88.13°
7:00:00	12.36°	98.02°
8:00:00	23.42°	108.68°
9:00:00	33.73°	121.11°
10:00:00	42.61°	136.54°
11:00:00	48.96°	156.1°
12:00:00	51.42°	179.31°
13:00:00	49.25°	202.65°
14:00:00	43.12°	222.5°
15:00:00	34.37°	238.17°
16:00:00	24.13°	250.76°
17:00:00	13.12°	261.52°
18:00:00	1.8°	271.45°
18:13:56	-0.833°	273.73°

Table 9a. Results from www.sunearthtools.com [52]

Date:	25/03/2016 | GMT-5	
Coordinates:	40.76, -73.984	
location:		
hour	Elevation	Azimuth
05:50:13	-1.071°	88.18°
6:00:00	0.78°	89.09°
7:00:00	12.11°	94.76°
8:00:00	23.14°	100.77°
9:00:00	33.41°	107.41°
10:00:00	42.24°	114.74°
11:00:00	48.52°	121.69°
12:00:00	50.94°	125.01°
13:00:00	48.78°	237.97°
14:00:00	42.69°	244.82°
15:00:00	33.98°	252.17°
16:00:00	23.77°	258.86°
17:00:00	12.77°	264.90°
18:00:00	1.45°	270.58°
18:13:56	-1.189°	271.88°

Table 9b. Results from the program developed.

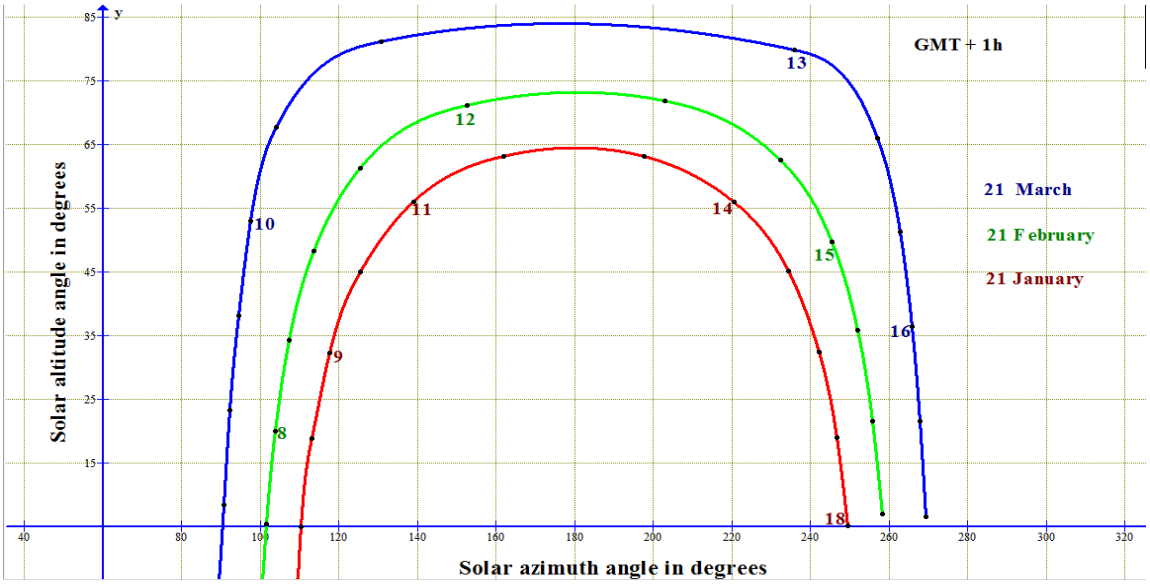

Fig. 6. Sun-path diagram for Bamenda, Cameroon.

7.Conclusion

This paper presented part II of a study aimed at predicting the GSR of some regions of Cameroon. Based on the Angstrom constants derived in part I of the study, the GSR of the intended Location is predicted and tabulated together with the statistical validation. The statistical methods used are: the mean bias error (MBE), the mean relative error (MRE), the root mean square error (RMSE) and t-statistic (t-stat) error. For better data modeling, these statistical error should be very close to zero.

From the above statistical analysis of the various models, graphs have been drawn and the variations of solar radiation values with months of the year analyzed. Although these statistical indicators generally provide a reasonable procedure to compare models, they do not objectively indicate whether a model's estimates are statistically significant, that is, not significantly different from their measured counterparts. In this study, an additional statistical indicator, the t-statistic was used. The statistical indicator allows models to be compared and at the same time indicate whether or not a model's estimates are statistically significant at a particular confidence level.

The results of this research indicate the main significance of developing empirical models for estimating the GSR on horizontal surfaces reaching the earth at different geopolitical zones in Cameroon. The developed models can also be applied to other location not considered and for places with similar climatic conditions with the determination of new empirical constants. The low MRE (0.0126 to 0.0422) and MBE (-0.2387 to 0.0144) exhibited by the proposed models imply they have good long-term representation of the physical problem. The RMSE values (0.2812 to 0.9198) indicates good agreement between the estimated and observed GSR while the t-stat values (0.012 to 1.3289) indicate reasonable statistically significance of the models' estimates at a particular confidence level.

It is observed that although the three models give reasonably good results as obtained from statistical analysis, the quadratic and cubic models give the closest results to the measured data for GSR with the cubic model being the overall best for estimation.

The best utilization of solar energy will be when the path of the sun can be tracked; hence an algorithm was implemented for tracking the sun position. Based on the algorithm, the solar position for Bamenda, for some days, is presented and results validated by those from sunearthtools. The solar position can be readily obtained, from the program developed, for other localities of interest.

The results if exploited can form the basis for developing and implementing solar energy systems for the entire nation of Cameroon and other regions of the world with similar geographical and climatic parameters.

References

[1] N. Emmanuel, T. Elie, Energy Systems:Vulnerability – Adaptation – Resilience (VAR), Helio International, Regional Focus: sub-Saharan Africa-Cameroon, 2009.

[2] D. Afungchui , N. Neba Rene, GSR of Some Regions of Cameroon using the linear Angstrom and non-linear Polynomial Relations (Part I) Model Development, International Journal of Renewable Energy Research, IJRER, vol. 3, issue 4, pp. 984-992, 2013.

[3] J. K. Page, The estimation of monthly mean values of daily short-wave radiation on vertical and inclined surfaces from sunshine records for latitude 40^0N – 40^0S, Proceedings of the UN Conference on New Sources of Energy, vol 4, pp. 378-390, 1964

[4] A. S. Angstrom, Solar and terrestrial radiation. Quart Journal of the Royal Meteorological Society, vol. 50, pp.121-126, 1924.

[5] E. O. Falayi and A. B. Rabiu. Modeling GSR using sunshine duration data. Nigeria Journal of Physics, vol. 17, pp.181-186, 2005.

[6] B. Safari and J. Gasore (2009). Estimation of GSR on horizontal surface in Rwanda using empirical models. Asian Journal of Science Research 2: 68-75.

[7] V. Badescu, Correlations to estimate monthly mean daily global solar irradiation: application to Romania. Energy, 24(10), pp.883-893, 1999.

[8] B. Aksoy (1997), Estimated monthly average global radiation for Turkey and its comparison with observations. Renewable Energy, vol. 10, pp.625-633, 1997.

[9] M. Sekar, M. Sakthivel, S. S. Kumar & C. Ramesh, Estimation of GSR for Chennai. European Journal of Scientific research, vol. 73(3), pp.415-424, 2012.

[10] H. Z. Che, G. Y. Shi, X. Y. Zhang, J. Q. Zhao, Y. Li, Analysis of sky condition using 40 years records of solar radiation data in China. Theoretical and Applied Climatology, vol. 89, pp.83-94, 2007.

[11] K. Ulgen and A. Hepbasli. solar radiation models. Part 2: Comparing and developing new models. Energy Sources, vol. 26, pp. 521-530, 2004.

[12] A. M. Al-Salihi, M. M. Kadum, and A. J. Mohammed, Estimation of GSR on horizontal surface using meteorological measurement for different cities in Iraq. Asian Journal of Scientific Research, vol. 3(4), pp.240-248, 2010.

[13] A. Sharma and B. Marwaha, Development of simulation weather data for Hour wise Daily Diffused and Direct Solar Radiation from Hourly Global Radiation using statistical estimation method for Subtropical region IJRER,Vol.5, No.4, 2015.

[14] R. J. Stone, Improved statistical procedure for the evaluation of solar radiation estimation models. Solar Energy, vol. 51(4), pp.289-291, 1993.

[15] L. E. Akpabio, S. O. Udo, S. E. Etuk, Empirical correlation of GSR with meteorological data for Onne,

Nigeria. Turkish Journal of Physics, vol. 28(3), pp.222-227, 2004.
[16] A. A. El-Sebaii, F. S. Al-Ghamdi, Al-Hazmi and Adel S. Faidah (2009). Estimation of GSR on horizontal surfaces in Jeddah, Saudi Arabia. Energy Policy, vol. 37, pp. 3654-3669, 2009.
[17] K. Bakirci, Correlations for estimation of daily GSR with hours of bright sunshine in Turkey. Energy, vol. 34, pp.485-501, 2009.
[18] R. T. Ogulata, S. N. Ogulata. Solar radiation in Adana, Turkey. Applied Energy, vol. 71, pp. 351-358, 2002.
[19] H. Aras, O. Balli and A. Hepbasli, Global Solar Potential. Part 1: Model Development. Energy Sources, Part B, vol. 1(3), pp. 303-315, 2006.
[20] K. Ulgen, A. Hepbasli , Estimation of solar radiation parameters for Izmir, Turkey. International Journal of Energy Resources, vol. 24, pp.773-785, 2002.
[21] B. G. Akinoglu, A. Ecevit , Construction of a quadratic model using modified Angstrom coefficients to estimate GSR. Solar Energy, vol. 45(2), pp.85-92, 1990.
[22] E. C. Okogbue, J. A. Adedokun, The estimation of solar radiation at Ondo, Nigeria , Journal of Physics, vol. 14, pp. 97-99, 2002.
[23] A. A. Trabea, M. A. M. Shaltout. Correlation of GSR with meteorological parameters over Egypt. Renewable Energy, vol. 21(2), pp. 297-308, 2000.
[24] M. S. Okundamiya and A.N. Nzeako, Estimation model for estimating solar radiation on horizontal surfaces for selected cities in the six geopolitical zones in Nigeria. Journal of Control Science and Engineering. Hindawi Publishing Corporation, 2011.
[25] A. Sfetsos, A. H. Coonick , Univariate and multivariate forecasting of hourly solar radiation with artificial intelligence techniques. Solar Energy, vol. 68:169-178, 2000.
[26] D. Njomo, L. Wald, Solar irradiation retrieval in Cameroon from meteosat satellite imagery using Helio_2 method. ISESCO Science and Technology Vision, vol. 2(1), pp. 19-24, 2006.
[27] M. Gunes, Analysis of daily total horizontal solar radiation measurements in Turkey. Energy Sources, vol. 23, pp. 563-570, 2001.
[28] A. Kilic, A. Ozturk , Solar Energy. Istanbul, Turkey: Kipas Distribution, 1983.
[29] H. Ogelman, A. Ecevit, and E. Tasdemiroglu, A new method for estimating solar radiation from bright sunshine data. Solar Energy, vol. 33, pp. 619-625, 1984.
[30] I. T. Togrul, H. Togrul, GSR over Turkey: Comparison of predicted and measured data. Renewable Energy, vol. 25, pp.55-67, 2002.
[31] M. Kaya, Estimation of GSR on horizontal surface in Erzincan, Turkey. International Journal of Physical Sciences, vol. 7(33) pp. 5273-5280, 2012.
[32] M. Sekar, M. Sakthivel, S. S. Kumar & C. Ramesh, Estimation of GSR for Chennai. European Journal of Scientific research, vol. 73(3), pp.415-424, 2012.
[33] A. M. Al-Salihi, M. M. Kadum, and A. J. Mohammed, estimation of GSR on horizontal surface using meteorological measurement for different cities in Iraq. Asian Journal of Scientific Research 3(4):240-248, 2010.
[34] T. D. M. A. Samuel, Estimation for GSR for Sri Lanka. Solar Energy, vol. 47, pp.333-337, 1991.
[35] S. Tarhan and A. Sari. Model selection for global and diffuse radiation over the Central Black Sea (CBS) region of Turkey. Energy Conversion and Management, vol. 46(4), pp. 605-613, 2005.
[36] E. Tasdemiroglu and R. Sever, Monthly and yearly average maps of total and direct solar radiation in Turkey. Solar Energy, vol. 37, pp. 205-213, 1986.
[37] E. Tasdemiroglu and R. Sever, Maps for average bright sunshine hours in Turkey. Energy Conversion and Management, vol. 31, pp.545-552, 1991.
[38] E. Tasdemiroglu and R. Sever, Estimation of monthly average daily diffuse radiation in Turkey. Energy, vol. 16, pp. 787-790, 1991.
[39] M. Tiris, C. Tiris and I. E. Ture , Diffuse solar radiations: Applications to Turkey and Australia. Energy, vol. 20, pp.745-749, 1995.
[40] M. Tiris, C. Tiris and I. E. Ture (1996). Correlations of monthly average daily global, diffuse and beam radiations with hours of bright sunshine in Gebze, Turkey. Energy Conversion and Management, vol. 37, pp. 1417-1421, 1996.
[41] K. Ulgen and A. Hepbasli, Comparison of solar radiation correlation for Izmir, Turkey. International Journal of Energy Resources, vol. 26, pp. 413-430, 2002.
[42] NASA, Surface Meteorology and Solar Energy Data and Information, 2010. http://eosweb.larc.nasa.gov/sse/,
[43] P. I. Cooper. The absorption of radiation in solar stills. Solar Energy, vol. 2(3), pp.333-346, 1969.
[44] J. A. Duffie, W. A. Beckman, Solar Engineering of Thermal Processes. John Wiley and Sons Inc. New York, 1991.
[45] United Nations. Department of peacekeeping operations. Cartographic Section. Map no. 4227, September 2004.
[46] Kipp & Zonen, Pyranometer Instruction Manual, 2000.
[47] M. Iqbal, An introduction to solar radiation. New York: Academic Press, 2003.
[48] H. Bulut and O. Buyukalaca . Simple model for the generation of daily GSR data in Turkey. Applied Energy, vol. 84, pp. 477-491, 2007.
[49] R. Saheli, Calculation of Sun Position and Tracking the Path of Sun for a Particular Geographical Location, 2012.
[50] DIN, DIN 5034 Part 2, Daylight in Indoor Rooms. Deutsches Institut für Normung e.V., Berlin, Beuth Press, 1985.
[51] V. Quaschning, Understanding Renewable Energy Systems, Earthscan, 2002.
[52] http://www.sunearthtools.com/ table of values consulted on 20/04/2016.
[53] Hanae Loutfi, Ahmed Bernatchou, Rachid Tadili, Generation of Horizontal Hourly Global Solar Radiation

From Exogenous Variables Using an Artificial Neural Network in Fes (Morocco), IJRER, Vol 7, No 3, 2017.

[54] N. Kumar, U. K. Sinha, S. P. Sharma, Y. K. Nayak, Prediction of Daily Global Solar Radiation Using Neural Networks With Improved Gain Factors and RBF Networks, IJRER, Vol 7, No 3, 2017.

[55] Paulinus Ekene Ugwuoke, Cajetan Ezeani Okeke, Statistical Assessment of Average Global and Diffuse Solar Radiation on Horizontal Surfaces in Tropical Climate , IJRER, Vol 2, No 2, 2012.

[56] Rami Al-Hajj; Ali Assi; Mohamad M. Fouad, A predictive evaluation of global solar radiation using recurrent neural models and weather data, 2017 IEEE 6th International Conference on Renewable Energy Research and Applications (ICRERA), Pages: 195 – 199, IEEE Conferences, 2017.

[57] Miguel Ángel Jiménez-Bello; Juan R. Castel; Luca Testi; Diego S. Intrigliolo, Assessment of a Remote Sensing Energy Balance Methodology (SEBAL) Using Different Interpolation Methods to Determine Evapotranspiration in a Citrus Orchard, IEEE Journal of Selected Topics in Applied Earth Observations and Remote Sensing, Volume: 8, Issue: 4, Pages: 1465 – 1477, IEEE Journals & Magazines, 2015.

[58] A Novel Application of Naive Bayes Classifier in Photovoltaic Energy Prediction, Ramazan Bayindir; Mehmet Yesilbudak; Medine Colak; Naci Genc, 2017 16th IEEE International Conference on Machine Learning and Applications (ICMLA), Pages: 523 – 527, IEEE Conferences, 2017.

[59] T. R. Ayodele; A. S. O. Ogunjuyigbe; E. O. Oyediran; Olorunfemi Ojo, Temperature based model for estimating the daily average global solar irradiation of Ibadan, Nigeria, AFRICON 2015, Pages: 1 – 5, IEEE Conferences, 2015.

[60] Kacem Gairaa; Farouk Chellali; Said Benkaciali; Youcef Messlem; Khellaf Abdallah, Daily global solar radiation forecasting over a desert area using NAR neural networks comparison with conventional methods, 2015 International Conference on Renewable Energy Research and Applications (ICRERA), Pages: 567 – 571, IEEE Conferences, 2015.